Photoacoustic Studies of $Cd_{1-x}Be_xSe$ Mixed Crystals[1]

J. Zakrzewski,[2,3] **M. Pawlak,**[2] **F. Firszt,**[2] **S. Legowski,**[2] **A. Marasek,**[2] **H. Meczynska,**[2] **and M. Malinski**[4]

This paper reports the results of photoacoustic measurements of $Cd_{1-x}Be_xSe$ mixed crystals grown by the high pressure Bridgman method with varying concentrations of Be $(0.1 < x < 0.2)$. For examining continuous wave photoacoustic spectra, a piezoelectric transducer (PZT) and an open cell were used. An increase of the energy gap with increasing x has been observed. The thermal diffusivity values were estimated using the dependence of the amplitude and phase of the PA signal on the light modulation frequency.

KEY WORDS: mixed crystals; piezoelectric detection; semiconductors.

1. INTRODUCTION

To account for the growing interest in wide gap ternary and quaternary II–VI semiconductor solid solutions, one has to involve their possible applications in optoelectronics [1]. Up to now the blue-green II–VI laser structures based on ZnSe and ZnCdSe are grown mainly on GaAs [2]. ZnSe-based compounds are found to cause a slow degradation of light-emitting diodes [3] and to shorten the lifetime of electroluminescent devices [4]. Recently, a new CdBeSe alloy has been used as an active layer material in green semiconductor lasers instead of ZnCdSe [5]. Because of dominant covalent bonding and the high cohesive energy of BeSe, one can anticipate a lattice strengthening of CdBeSe, as compared with ZnCdSe, as

well as the possibility of obtaining lattice-matched material to GaAs and ZnSe structures [6,7]. Thus far, studies have focused mainly on molecular beam epitaxy (MBE) grown $Cd_{1-x}Be_xSe$, while the physical properties of respective bulk compounds remain virtually unknown [8]. For samples of MBE-grown $Cd_{1-x}Be_xSe$, the best optical and structural properties have been observed in the vicinity of $x = 0.46$ [9]. An estimated band gap bowing parameter for this material is about 3 eV and indicates strong bowing [5].

This paper presents preliminary results of photoacoustic and photoluminescence measurements of $Cd_{1-x}Be_xSe$ crystals grown from CdSe, Be, and Se melts by the modified Bridgman method.

2. EXPERIMENT

The crystals were grown by the high-pressure Bridgman method under argon overpressure (14 MPa), and were cut into plates 1–1.5 mm thick. They were then mechanically polished and chemically etched. The investigated crystals were of the wurtzite-type structure.

Photoacoustic (PA) measurements were carried out using an open cell. A xenon lamp (Cermax 300 W) and He–Cd laser (325 nm) were employed as excitation sources for PA spectra and thermal diffusivity measurements, respectively. A piezoelectric transducer (PZT) and lock-in amplifier (Stanford SR 510) were applied to detect the PA signal using a wave conversion method. All measurements were performed at room temperature.

Luminescence spectra were measured in a spectral range from 350 to 800 nm, under He–Cd laser (325 nm) excitation, in the temperature range from 33 K to room temperature.

3. RESULTS

Photoacoustic investigations were performed on samples of CdSe and $Cd_{1-x}Be_xSe$ ($x = 0.1$ and $x = 0.2$) crystals. Figure 1 shows the spectra of CdSe at three different frequencies. Two maxima are observed in the energy range 1.6–1.85 eV for the amplitude spectra. For all frequencies, the maximum appeared in the sub-band-gap region, and its position, contrary to the prediction of the Jackson–Amer theory, did not depend on the modulation frequency [10]. Because of compensation for bending and expansion of samples due to heating, the PZT transducer situated behind the sample registered an amplitude signal that goes to zero at $\alpha l = 2$. The ratio of peak intensities in the high and low absorption regions decreases with an increase of the modulation frequency.
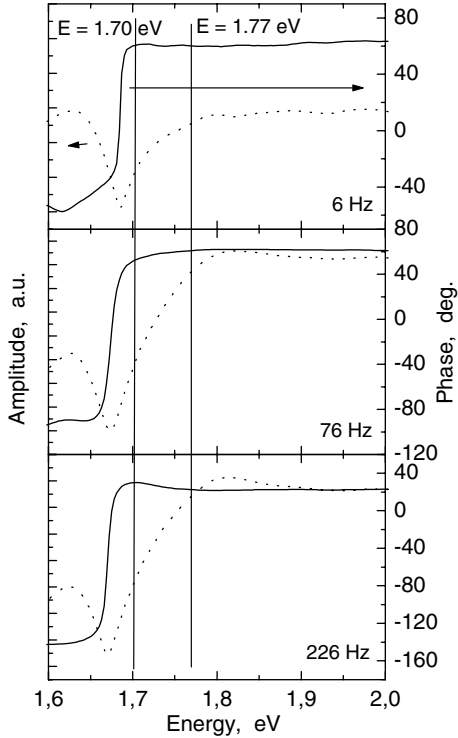
Fig. 1. Phase (solid) and amplitude (dots) spectra of CdSe for different modulation frequencies.

Since the general expression for the PA signal is complicated, it is difficult to find the relation between the amplitude and phase of the PA signal, and the absorption coefficient. In previous papers we considered the case of a thermally thin but optically thick sample, which was correct for spectra in the high absorption region where saturation or an amplitude decrease appears for the amplitude spectra. In the phase spectra, the value of the signal in the high absorption region becomes constant for values of energies higher than the energy gap. This feature was used to determine E_g. For CdSe the energy gap was estimated at $E_g = 1.77$ eV, which agrees with literature data.

At an energy of $E = 1.70$ eV, the bending point—the change of the slope in amplitude spectra—can be clearly seen. The change in the phase value could be linked to the changing character of photoacoustic signal generation, as was seen for $Cd_{1-x}Mn_xTe$ [11]. Such experimental curves

features in the energy range $1.70\,\text{eV} < E < 1.77\,\text{eV}$ could be associated with the absorption edge – the Urbach tail.

Two samples (labeled a and b) were measured with a beryllium content of 10% in the ingot (starting material). The amplitude and phase spectra for different modulation frequencies are presented in Fig. 2 (sample a) and Fig. 3 (sample b). The value of the energy gap for the sample a was determined as $E_g = 1.88\,\text{eV}$ from the phase spectra. The bending point was also observed in the amplitude spectra for this energy value. The character of the phase spectra for the sample b, however, was very different. Two characteristic points could be singled out for energies $E = 1.78$ and $1.91\,\text{eV}$, the latter value corresponding to the energy gap. That region, too, could be associated with the absorption edge, as was observed for CdSe.

Figure 4 shows the amplitude and phase spectra of the $Cd_{1-x}Be_xSe$ sample with a beryllium content of 20% in the ingot. In this case, two

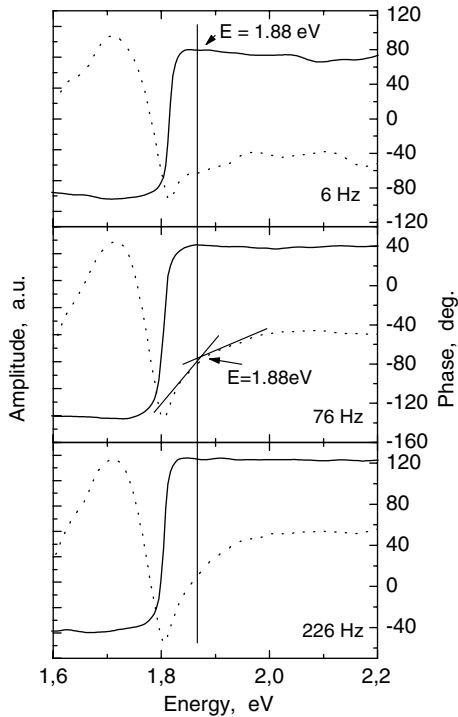**Fig. 2.** Phase (solid) and amplitude (dots) spectra of $Cd_{1-x}Be_xSe$ ($x = 0.1$, sample a) for different modulation frequencies.

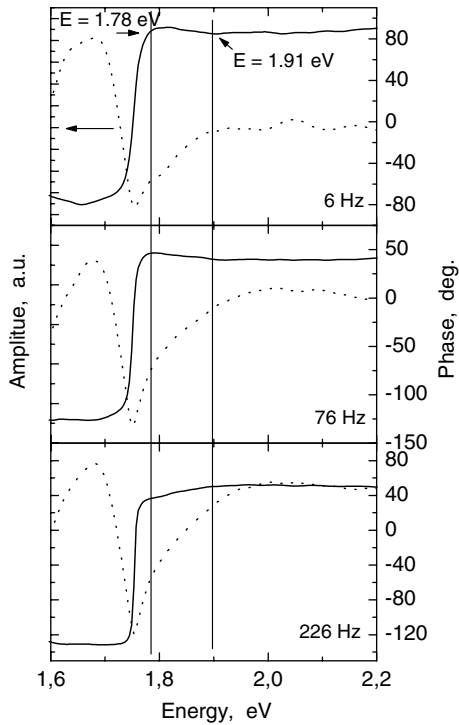**Fig. 3.** Phase (solid) and amplitude (dots) spectra of $Cd_{1-x}Be_xSe$ ($x = 0.1$, sample b) for different modulation frequencies.

characteristic points were noted for energies $E = 1.81$ and $1.93\,eV$ (the latter being the value of the energy gap). As the above data show, the energy gap increases with an increase of beryllium content.

Figure 5 gives the photoluminescence (PL) spectrum of $Cd_{0.9}Be_{0.1}Se$ (sample a) at $T = 33\,K$. The high-energy part of the spectrum exhibits two peaks positioned at 1.956 and 1.85 eV. The second one, thermally quenched at a temperature higher than 100 K, is interpreted as an "edge emission" due to recombination of shallow donor–acceptor pairs. The first line, observed as high as room temperature, shifts monotonically towards lower energies with increasing temperature, and is interpreted as an exciton emission. Its maximum at room temperature appears at an energy of 1.866 eV, which corresponds very well to the ellipsometric data (1.865 eV).

Because the photoacoustic signal depends on heat diffusion in the sample, it is possible to use the PA method to study the thermal properties
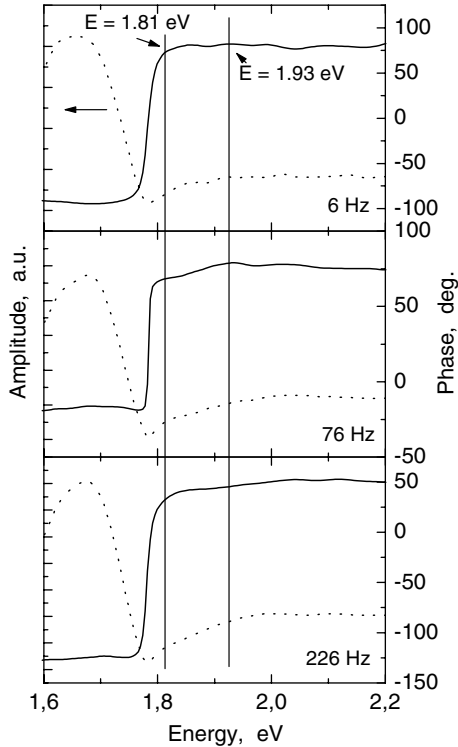
Fig. 4. Phase (solid) and amplitude (dots) spectra of $Cd_{1-x}Be_xSe$ ($x = 0.2$) for different modulation frequencies.

of semiconductors. Thermal diffusivity represents the rate of heat diffusion in the material, and is a phenomenological parameter such as the absorption coefficient. Thermal diffusivity values for $Cd_{1-x}Be_xSe$ were determined using photoacoustic amplitude and phase signals dependence on modulation frequency. The model developed by Blonskij et al. [12] was applied. This study averaged the thermal diffusion equations over the area of the sample, solved the thermoelastic problem, and provided analytical expressions for the amplitude and phase, namely,
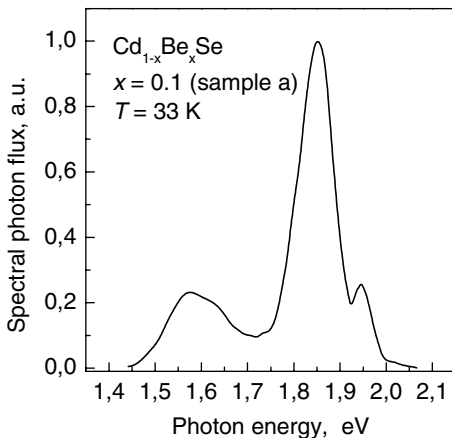
$$|V| = \frac{P\alpha}{kla^2}\psi(al), \tag{1}$$

Fig. 5. Luminescence spectra of $Cd_{1-x}Be_xSe$ ($x = 0.1$, sample a) for temperature $T = 33$ K.

$$\psi(al) = \left\{ \left[1 - \frac{3}{2al} \frac{\sinh(al) + \sin(al)}{\cosh(al) + \cos(al)} \right]^2 \right. $$
$$\left. + \left[\frac{3}{2al} \frac{\sinh(al) - \sin(al)}{\cosh(al) + \cos(al)} \right]^2 \right\}^{1/2} \qquad (2)$$

$$\tan\tilde{\varphi} = \frac{\dfrac{3}{2al} \dfrac{\sinh(al) - \sin(al)}{\cosh(al) + \cos(al)}}{1 - \dfrac{3}{2al} \dfrac{\sinh(al) + \sin(al)}{\cosh(al) + \cos(al)}}, \qquad (3)$$

where V, φ are the amplitude and phase signals, respectively, α is the absorption coefficient, k is the thermal conductivity, l is the sample thickness, P is a constant, $a = \sqrt{\omega/2D}$, $\omega = 2\pi f$, f is the modulation frequency, and D is the thermal diffusivity.

Figure 6 shows the dependence of the $\psi(al)$ term on the square root of the modulation frequency for three samples of $Cd_{1-x}Be_xSe$ ($x = 0.1$, samples a and b; $x = 0.2$). The CdSe sample with a known value of thermal diffusivity ($D = 0.061$ cm²·s⁻¹) was used to calibrate the measurements. The obtained values of the thermal diffusivities are $D = 0.02$ cm²·s⁻¹ for $Cd_{1-x}Be_xSe$ ($x = 0.1$, sample a), $D = 0.09$ cm²·s⁻¹ for $Cd_{1-x}Be_xSe$ ($x = 0.1$, sample b), and $D = 0.01$ cm²·s⁻¹ for $Cd_{1-x}Be_xSe$ ($x = 0.2$).
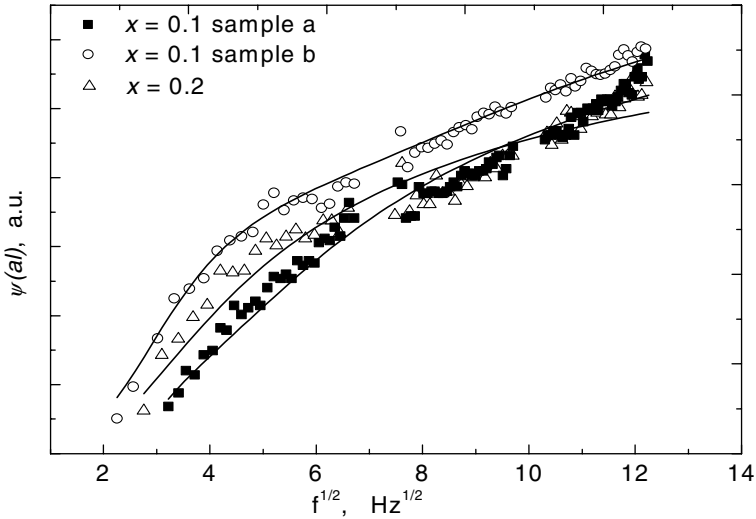
Fig. 6. Dependence of $\psi(al)$ term on square root of modulation frequency for three samples of $Cd_{1-x}Be_xSe$ ($x = 0.1$, samples a and b; $x = 0.2$). Solid line = fitted curve.

Because the setup used in the experiment differed slightly from the one used in the Blonskij model, modification of the experimental system is in progress in order to improve the accuracy of those measurements.

REFERENCES

1. G. Landwehr, *Proc. Second Int. Symp. Blue Lasers and Light Emitting Diodes*, (Chiba, Japan, 1998), p. 3.
2. H. Morkoc, S. Strite, G. B. Gao, M. E. Lin, B. Sverdlov, and M. Burns, *J. Appl. Phys.* **76**:1363 (1994).
3. K. Nakamo and A. Ishibashi, *Mater. Sci. Forum* **1329**:258 (1997).
4. E. Kato, H. Noguchi, M. Nagai, H. Okuyama, S. Kijima, and A. Ishibashi, *Electron. Lett.* **34**:282 (1998).
5. S. V. Ivanov, A. A. Toporov, T. V. Shubina, A. V. Lebeder, S. V. Sorokin, A. A. Sitnikova, P. S. Kop'ev, G. Reusher, M. Kein, F. Bensing, A. Waag, G. Landwehr, G. Pozina, J. P. Bergman, and B. Monemar, *J. Cryst. Growth* **214/215**:109 (2000).
6. Ch.Verie, in *Semiconductor Heteroepitaxy Growth, Characterization and Device Applications*, B. Gill and R. L. Aulombard, eds. (World Scientific Pub. Co., Singapore, 1995), p. 73.
7. A. Waag, F. Fisher, K. Schuell, T. Baron, H. J. Lugauer, Th. Litz, U. Zehnder, W. Ossau, T. Gerhardt, M. Kein, R. Reuscher, and G. Landwehr, *Appl. Phys. Lett.* **70**:280 (1997).
8. S. V. Ivanov, A. A. Toropov, T. V. Schubina, S. V. Sorokin, O. V. Nekrutkina, V. A. Kaygorodov, P. S. Kopev, G. Reuscher, M. Kein, A. Waag, and G. Landwehr, *Phys. Stat. Sol. A* **180**:275 (2000).

9. M. Kein, M. Korn, F. Bensing, A. Waag, G. Landwehr, S. V. Ivanov, S. V. Sorokin, A. A. Sitnikova, T.V. Schubina, and A. A. Toropov, *J. Cryst. Growth* **214/215**:684 (2000).
10. J. W. Jackson and N. M. Amer, *J. Appl. Phys.* **51**:3343 (1986).
11. J. Zakrzewski, F. Firszt, S. Legowski, H. Meczynska, M. Pawlak, and A. Marasek, *Rev. Sci. Instrum.* **74**:566 (2003).
12. I. V. Blonskij, V. A.Thoryk, and M. L. Shendeleva, *J. Appl. Phys.* **79**:3512 (1996).